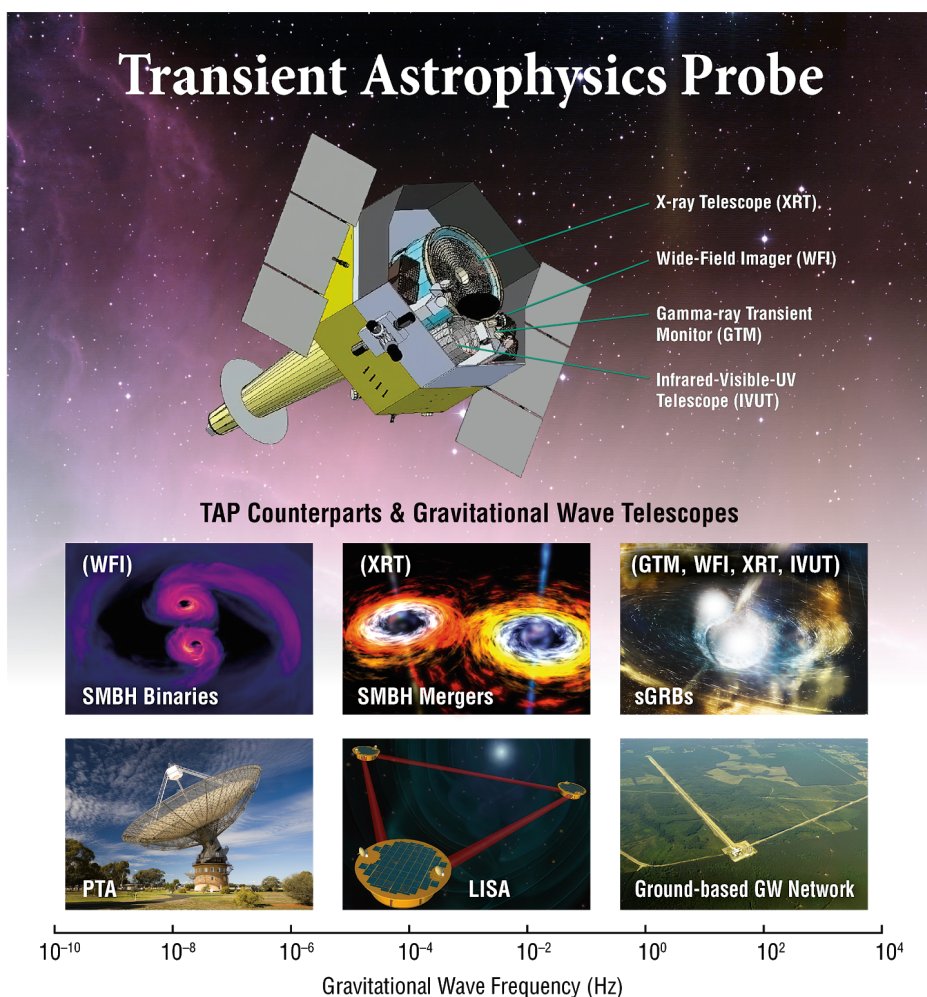


Transient Astrophysics Probe

White Paper

Lead author: Jordan Camp, NASA-GSFC, 301-286-3528, jordan.b.camp@nasa.gov

Josh Abel (GSFC), Scott Barthelmy (GSFC), Mark Bautz (MIT), Ehud Behar (Technion), Edo Berger (Harvard U), Sarah Spolaor (W Virginia U), S. Brad Cenko (GSFC), Neil Cornish (Montana St U), Tito Dal Canton (GSFC), Chris Fryer (LANL), Suvi Gezari (U Md), Paul Gorenstein (SAO), Sylvain Guiriec (GWU), Dieter Hartmann (Clemson U), Vicky Kalogera (NW U), Chryssa Kouveliotou (GWU), Jeffrey Kruk (GSFC), Alexander Kuttyrev (GSFC), Raffaella Margutti (NW U), Francis Marshall (GSFC), Brian Metzger (Columbia U), Cole Miller (U Md), Scott Noble (GSFC), Jeremy Perkins (GSFC), Andrew Ptak (GSFC), Bill Purcell (Ball Aerospace), Judith Racusin (GSFC), Josh Schlieder (GSFC), Jeremy Schnittman (GSFC), Alberto Sesana (U Birmingham), Peter Shawhan (U Md), Leo Singer (GSFC), Alex van der Horst (GWU), Richard Willingale (U Leicester), Kent Wood (NRL), William Zhang (GSFC)



1. Executive Overview

The Transient Astrophysics Probe (TAP, *URL 1*) is a multi-wavelength observatory that will greatly advance our understanding of the transient Universe. TAP will feature the characterization of electromagnetic (EM) counterparts to Gravitational Waves (GW) involving mass scales from neutron stars (NS) to $10^9 M_{\odot}$ Supermassive Black Hole (SMBH) Binaries. TAP will also target a broad range of time-domain astrophysical phenomena involving compact objects. To reach these goals, we propose a multi-instrument platform, enabling high-sensitivity transient discovery as well as rapid follow-up over a broad energy range. Wide-field X-ray and gamma-ray monitors, a wide-field, sensitive X-ray telescope, and a wide-field, sensitive IR/optical/UV telescope comprise the complementary instrument suite (§4). TAP needs only one modest (currently funded) technology development (§5), and fits in the Probe \$1B cost cap (§8).

The most exciting avenue of investigation in the TAP discovery space will be the astrophysical characterization of GW events (Tables 1, 2). The TAP X-ray and IR-optical-UV instruments will provide an optimal means for follow-up and localization of GW detections by the LIGO-Virgo-KAGRA-LIGOIndia network, as well as X-ray follow-up of detections from the space-based GW observatory LISA. Counterparts to very massive GW sources identified by Pulsar Timing Arrays (PTAs) are also likely to be detectable with TAP’s all-sky X-ray survey. TAP will follow up GW events spanning the BH range from a few to billions of M_{\odot} . The scientific output will be prodigious, including insights in cosmology, nucleosynthesis, interactions of merging accretion disks, the engines of gamma-ray bursts (GRBs), and tests of magnetohydrodynamic/General Relativity models of merging compact objects.

In addition, TAP will address a multitude of transient astrophysical phenomena associated with compact objects in a large range of environments: cosmic explosions (GRBs, Supernovae), and the launch and acceleration of matter in relativistic jets (Active Galactic Nuclei (AGN), Tidal Disruption Events (TDEs); Table 2). Through its support of a broad Guest Observer community in targeted as well as follow-up time-domain observations (Fig. 1), TAP can be described as a “next generation *Swift* observatory”, with each of its instruments achieving a factor ~ 10 improvement relative to the corresponding *Swift* instrument (Table 4).

When TAP is not chasing newly discovered transients (onboard or following up sources from other facilities), it will conduct a broadband sky survey (Fig. 1, §4.1). Finally, there will be considerable synergy in the time-domain X-ray and IR-UV observations afforded by TAP with other time-domain facilities including LSST (optical), and LOFAR and SKA (radio).

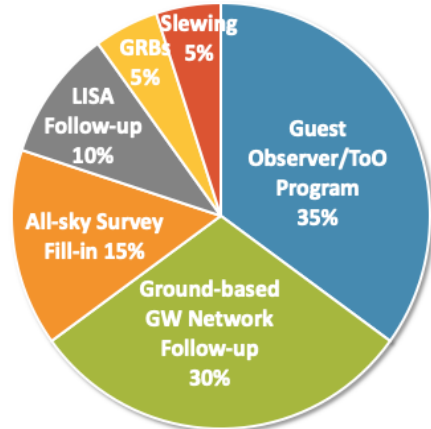


Figure 1: TAP has a diverse observing program with key science goals: GW follow-up, high- z GRBs, filling in X-ray sky survey, Guest Observer program.

2. Science Goals and Objectives

2.1 Gravitational Wave Counterparts

The timescales and observing scenarios for electromagnetic counterparts to GW signals differ widely across the GW spectrum. The best understood targets are binary NS mergers observed by the kilohertz-band ground-based interferometers, and these events drive the TAP design. However, TAP's versatility makes it a powerful facility to search for counterparts in the millihertz band LISA signals and nanohertz band PTA signals. TAP provides comprehensive coverage of NS mergers, and the flexibility to search for counterparts across the GW spectrum.

2.1.1 LIGO-Virgo-KAGRA-India (Ground-based GW Network)

By the late 2020s, a worldwide network of ground-based GW detectors will discover hundreds of compact binary mergers per year [Abbott 2018]. Although the GW data alone will provide many details of the sources - the masses, and possibly the spins - it will perform a very limited probe of the environment and the baryonic and electromagnetic processes associated with the sources. Moreover, the GW data will localize the sources with limited precision; a focused EM signal is necessary to localize the host galaxy of the GW event. Many of the GW events will involve at least one NS and will emit EM radiation over a wide range of wavelengths. Therefore, EM observations will be necessary to place the events in their full astrophysical context and complete the picture of each future detection [Sathyaprakash, 2019], [Burns, 2019].

TAP observations, in combination with ground-based follow-up EM observations, will break parameter degeneracies, independently establish source distances and energy scales, illuminate jet astrophysics, find r-process nucleosynthesis sites, and reveal host galaxies. The discovery of the binary neutron star (BNS) merger GW170817 [Abbott 2017b] suggests that three kinds of EM counterparts will accompany future BNS discoveries from ground-based GW detectors: short GRBs [Abbott 2017c], X-ray afterglows [Troja 2017], and kilonovae [Metzger 2018]. These are the main drivers of the TAP design (see §4), which include 1) a wide-field X-ray imaging telescope (WFI) with a 0.4 sr FoV, sufficiently large to efficiently tile the GW skymap (area $<1000 \text{ deg}^2$) when two or more of the five GW detectors are operating; 2) a sensitive IR-visible-UV telescope (IVUT) with 1 deg^2 FoV that will follow up the UV to IR kilonova emission when four or more GW detectors are operating (skymap area $<30 \text{ deg}^2$); 3) a sensitive X-ray telescope (XRT) with 0.8 deg^2 FoV to search for on- and off-axis X-ray emission when four or more GW detectors are operating; and 4) an all-sky gamma-ray transient monitor (GTM) to search for on- and off-axis gamma-ray emission for all GW detections.

In **Table 1**, TAP counterpart detection rates and timescales are shown, using the LIGO A+ upgrade sensitivity of 323 Mpc range for BNS mergers (URL 2), and a volumetric rate of BNS mergers of $1000 \text{ Gpc}^{-3} \text{ yr}^{-1}$. The detection efficiency and rate of the different counterparts are simulated by using the expected counterpart signal flux, and the detector sensitivities listed in **Table 3**. For off-axis gamma-ray, X-ray, IR and UV signals we use the fluxes obtained from the

multi-wavelength counterpart study of GW170817, along with its observed distance of 40 Mpc, to find the detection efficiency, and associated counterpart detection rate within the enhanced GW horizon. For on-axis gamma-ray and X-ray counterparts, we use the set of prompt gamma-ray and afterglow X-ray fluxes with known redshift measured by *Swift*, scaled to the enhanced GW horizons, and include a beaming factor of 0.06 [Fong, 2015].

The resultant high detection rates of **Table 1** will allow detailed studies of populations of the range of Ground-based GW Network counterparts.

Table 1: *GW Ground-Based Network Counterparts and associated rates measured by TAP.*

Counterpart Bandpass	Detector	Counterpart ¹	Enhanced BNS GW Horizon ²	Counterpart Detection Efficiency	Counterpart Detection Timescale	Counterpart Detection Rate (yr ⁻¹)
Gamma-ray	GTM	Prompt on-axis	485 Mpc	0.8	sec	20
Gamma-ray	GTM	Prompt off-axis	323 Mpc	0.01	sec	2
X-ray	WFI	Afterglow on-axis	485 Mpc	0.75	min	20
X-ray	XRT	Afterglow on-axis	485 Mpc	0.9	min	14
X-ray	XRT	Afterglow off-axis	323 Mpc	0.1	weeks	7
UV	IVUT	Kilonova	323 Mpc	0.8	hour	56
Optical/IR	IVUT	Kilonova	323 Mpc	1	days	70

1. An off-axis or kilonova counterpart is assumed to have the luminosity associated with GW170817.
2. The GW horizon is enhanced for on-axis orientation by a peaking of the GW amplitude along the jet axis.

2.1.2 LISA Counterparts

Unlike stellar-mass BHs, which are expected to reside in gas-poor environments, there is substantial theoretical motivation for there to be significant gas nearby, and thus EM counterparts to, the massive BH binaries formed at the centers of merging galaxies [Baker, 2019]. With the space-based interferometer LISA, we expect to see GWs from relatively lower-mass systems (10^6 - $10^7 M_{\odot}$). With coordinated observations from LISA, TAP will utilize an early-warning system that will give error boxes on the order of a few square degrees as much as several days before the binary BH merger. This will allow phase-sensitive observations [Haiman 2017] with the XRT/IVUT. For SMBH binaries with non-trivial amounts of gas in the vicinity, prompt signatures are likely [D’Ascoli 2018]. They will have peak luminosities comparable to TDEs (many times Eddington), with signals varying over a few dynamical times near merger.

With an EM counterpart detected by XRT, the host galaxy for the LISA signal can be identified. Measuring the host galaxy redshift opens up a wide variety of possible science, testing fundamental physics and cosmology. Depending on the specific formation mechanisms responsible for $z < 3$ SMBH, we expect to detect and localize several of these sources with LISA and TAP coordinated observations spanning a 5 yr mission [Dal Canton 2019], assuming operational overlap of the missions. These observations will provide strong constraints on the

leading models of BH formation and evolution in cosmic time. A number of assumptions in [Dal Canton 2019] are conservative, and the actual detection rates may be substantially higher.

2.1.3 Pulsar Timing Array (PTA) Counterparts

SMBH binaries are the most energetic GW sources in the Universe. The systems most likely to be detected with PTAs will have particularly high masses ($\gtrsim 10^8 M_\odot$), long periods ($T_{\text{orb}} \gtrsim 1$ yr), and reside in the local Universe ($z \lesssim 1$). As a population, these sources are expected to combine to produce a stochastic signal at nanohertz frequencies, with characteristic strain amplitude around $h \sim 10^{-15}$. At the current rate of PTA improvements, the stochastic background could very well be detected by 2024 [Taylor 2016]. The first individually resolvable sources should be detectable shortly thereafter, and will mostly likely represent the high-mass, short-period systems - the most nearby outliers from the stochastic population. Based on the steadily improving sensitivity of PTAs and the expected occupation fraction of SMBH binaries in the local Universe, by the year 2030 we expect at least a handful of binary SMBHs to be detected and individually resolved by PTAs (Mingarelli 2017). Simulations of modulated X-ray emission from these relatively close sources (within 1 Gpc), with period ~ 1 year, lead us to expect several WFI detections of EM counterparts to PTA sources over the course of the mission, observed with the WFI in weekly integrations [Schnittman 2014].

Eventually, PTA detections will provide a direct measurement of the GW phase and frequency of a binary, which are among the more critical parameters in direct counterpart identification. PTA measurements will still have degeneracies in mass, distance, and eccentricity. Identifying the host galaxy of such a system can break the mass/distance degeneracy through a redshift measurement, and thus allow a precision mass measurement for the binary that can be directly compared to host galaxy properties. The identification of clear counterpart signatures at any waveband will both contribute to studying these objects as multi-messenger targets, and serve as a “Rosetta Stone,” allowing existing and future surveys to identify and study a vast population of binary systems previously unidentified as SMBH binaries [Kelley, 2019].

2.2 Time-Domain Astronomy

With the 2020s bringing about an era of wide-field survey telescopes across the EM spectrum (LSST in optical, WFIRST in NIR, SKA in radio), a high-energy counterpart discovery machine like TAP is needed to both *detect* and *follow up* transient and variable sources in cooperation with these other facilities. In this section we describe a subset of the time-domain science possible with TAP, and list predicted source discovery rates in **Table 2**.

2.2.1 High-Redshift GRBs and the Epoch of Reionization

The 2010 Decadal Survey identified the “[search] for the first stars, galaxies, and black holes” as the highest priority scientific objective for the current decade. Of particular importance is to understand the timescale and source population responsible for cosmic reionization. GRBs serve as unique probes of this critical era in the evolution of the Universe [Grindlay 2019].

Because their afterglows are very bright, GRBs have been detected out to redshift 8–9 [Tanvir 2009, Cucchiara 2011]; given their simple power-law energy spectra, GRBs serve as a probe of high-redshift Lyman break galaxies, as they reveal galaxies independent of host luminosity.

The rate and population distributions of long duration GRBs was derived from an intrinsic sample developed for evaluation of the *Swift*-BAT sample in [Lien 2014]. Simulations includes both paths to GRB detection: GTM detection followed by WFI tiling in search of the afterglow, and detection by the WFI of the prompt emission and/or ongoing afterglow during the survey and other targeted observations. The simulations indicate a detection rate of ~ 25 per year at $z > 5$, and several per year at $z > 8$. Detections with the WFI will be followed by IVUT observations to determine redshift, spectra, light curves, and positions.

2.2.2 Tidal Disruption Events

When a star is scattered into the tidal radius of a SMBH, tidal forces will tear the star apart. For BHs less massive than $10^8 M_{\odot}$, the bound debris will accrete and emit a flash of radiation [TDE; Rees 1988]. TDEs serve as signposts, pointing the way towards SMBHs in distant galaxies that may not otherwise be detectable.

Discovery and follow-up of TDEs in the UV and soft X-ray bands promises to substantially increase the sample size, providing population level analyses of this source class. The known TDEs can be separated into highly luminous jetted events [Burrows 2011], and non-jetted events (where the jet is pointed away from us).

2.2.3 Supernova Shock Breakouts

Supernovae (SNe) are critical to our understanding of a variety of topics in modern astrophysics. Type Ia SNe, the thermonuclear explosion of a white dwarf, are used as standardizable candles for precision cosmology, having provided the first evidence for the accelerating expansion of the Universe [Riess 1998, Perlmutter 1999]. With their massive star progenitors, core-collapse SNe are responsible for the production of heavy elements and high-energy cosmic rays, and also regulate galaxy growth via feedback. However, more than half of these cosmic explosions lack robust progenitor identifications, limiting our understanding of topics ranging from stellar evolution to dark energy.

TAP will provide unique discovery space in ccSNe Shock Breakouts. These rare, short lived (hundreds of seconds) transients provide the precise time of the SN, and also important physics about the progenitors, including radius, mass loss history, and composition. They will be detected by the WFI, XRT and IVUT during survey pointings longer than the transient duration.

2.2.4 Active Galactic Nuclei

Type I AGN are understood to be unobscured accreting SMBHs with a direct line of sight to their central engine, characterized by a strong X-ray component (typically $>10\%$ of the bolometric luminosity) and variable over a wide range of timescales [Beckmann 2012], from hours to years. Historically, AGN light curves have come from intensive, targeted campaigns

focused on a few bright sources [McHardy 2006; Körding 2007]. Joint X-ray and optical/IR monitoring also probes emission reprocessing mechanisms and the geometry of the central engine [Breedt 2010]. The WFI will be able to monitor ~ 500 of these bright AGN on a weekly basis, and the brightest ~ 80 of these on a daily basis. The XRT will detect many more at lower flux levels. One of the main science results that would emerge from such a large, unbiased time-domain survey of AGN is a much-improved understanding of their range of variability and classes. This will allow us to quantify the significance of any periodic signals seen in these light curves, in turn identifying binary SMBH candidates for more detailed multi-wavelength study.

2.2.5 Synergy with other Time-Domain Facilities: LSST and SKA

TAP has a myriad of synergies with the wide-field time-domain surveys that will revolutionize astronomy in the 2020s. LSST will generate transient and variable alerts at an astounding rate: $\sim 10^6$ new astrophysical transients each night. TAP can provide multi-wavelength context to help classify a subset of new LSST transients: for example, the presence/absence of a contemporaneous GRB will help differentiate on-axis from orphan afterglows, while past X-ray variability can help distinguish AGN from TDEs. For the most interesting LSST transient discoveries, TAP can provide prompt (\sim minutes), multiwavelength *follow-up* to assist with characterization. TAP will also conduct daily *co-observing* of an LSST “deep drilling” field to perform broadband reverberation mapping measurements of bright AGN.

2.2.6 Additional TAP Science

TAP’s powerful suite of instruments will enable a host of additional transient science, including observations of blazars, GRBs, NS thermonuclear bursts, dust-enshrouded IR transients, exoplanet IR characterization, M star flares, and neutrino counterparts. In addition newly discovered source classes are likely from its high sensitivity all-sky X-ray survey.

2.3 Source Rates

Table 2: *Estimated rates of sources discovered by the TAP instruments.*

Transient Type	WFI Rate (yr ⁻¹)	XRT Rate (yr ⁻¹)	IVUT Rate		GTM rate (yr ⁻¹)
			IR (yr ⁻¹)	UV (yr ⁻¹)	
Objective 1 – X-ray, UV and IR Counterparts to Gravitational Wave Sources					
GW NS-NS (on-axis)	20	14	--	--	20
GW NS-NS (off-axis)	--	7	70	56	2
GW SMBH-SMBH ($10^6 M_{\odot}$)	--	≥ 1	--	--	--
GW SMBH-SMBH ($10^9 M_{\odot}$)	Several in 5 yr	--	--	--	--
Objective 2 - Highest Sensitivity Time-Domain Survey of the Transient Soft X-ray / UV Sky					
ccSN shock breakout	1	19	--	6	--
Jetted TDEs	106	1	--	--	--
Non-jetted TDEs	1	48	--	40	--
AGN (daily / weekly)	120 / 660	1600 / 8700		--	--
High-z GRBs ($z > 5$)	25	--	22	--	--

3. Mission and Spacecraft Metrics

The 4 TAP instruments are mounted on the spacecraft bus (see **cover image**). The orbit is a Sun-Earth L2 Halo. The total mission (spacecraft bus + instruments) expected (CBE) and maximum (MEV) mass is 1512 / 1952 kg, power 1274 / 1636 W, and telemetry 6.3 / 8.3 Gbyte/day (contingencies run 28.1 to 31.2%). The bus pointing stability is 10 arcsec over 1500 sec. The bus can slew 70° in 50 sec including settling. Mission life is 5 yrs with a goal of 10 yrs.

4. Instrumentation Payload

4.1 Instrument Requirements and Concept of Operations

The TAP instrument suite is comprised of the WFI, XRT, IVUT, and GTM (see **cover image**); **Table 3** lists the requirements. TAP's L2 orbit provides a thermally stable environment and minimizes Earth occultation; 3 or 4 equally-spaced dedicated ground stations enable full time, low-latency (seconds) uplink and downlink connections. Positions, lightcurves, and spectra are sent within minutes of detection of a transient. When not responding to ToOs, the 3 imaging instruments are in survey mode (~30 regions per day, giving ~daily WFI full-sky coverage).

Table 3: TAP instrument parameter requirements.

Parameter	WFI	XRT	IVUT	GTM
FoV	36.2x36.2° (0.4 sr)	1° dia	1x1° (sq)	4 π sr
Aperture Size	35x35 cm (each module)	130 cm dia; fl=500 cm	70 cm dia	20 cm dia / det
PSF/FWHM	9 arcmin	5 arcsec HPD	0.22 arcsec	10° radius [1]
Energy Range	0.4 - 5 keV	0.2 - 10 keV	0.2 - 2.5 μm	10 keV - 1 MeV
Sensitivity	2x10 ⁻¹¹ erg/sec cm ² (2 ks)	5x10 ⁻¹⁵ erg/sec cm ² (2 ks)	23 mag (300 s)	0.9 ph/cm ² /s [2]
Mass (CBE/MEV)	159 / 207 kg	294 / 382 kg	135 / 176 kg	53 / 69 kg
Power (CBE/MEV)	276 / 359 W	370 / 481 W	119 / 155 W	48 / 63 W
Data (CBE/MEV)	5 / 6.5 GB/day	0.3 / 0.4 GB/day	0.8 / 1.1 GB/day	0.15/0.2 GB/day
TRL	6	5 (6 by 2021)	6	6

[1] For GTM this is a localization metric, not a PSF. [2] Sensitivity in the 50-300 keV band in 1 sec.

4.2 Wide-Field Imager (WFI)

Sensitivity: Each WFI module has micro-channel optics (MCO) that produce an X-ray image on the CCD detector plane. A 45-cm focal length MCO array yields 0.4 sr FoV coverage (4 modules), and localization of ~1 arcmin. The sensitivity is 2x10⁻¹¹ ergs s⁻¹ cm⁻² in 2 ks in the 0.4-5 keV band (based on ray tracing to measure the effective area, laboratory measurements of the MCO, and for background (a) a power-law background to represent the cosmic diffuse X-ray background, (b) a thermal model for the Galactic X-ray background, and (c) the particle background). **MCOs:** These optics [Angel 1979] provide constant imaging performance and effective area across the entire FoV. The optic consists of microscopic square channels extending radially from a spherical surface manufactured in glass, focusing the X-rays into a cross-like

pattern with a central core. With an 8x8 array of tiles (1 module), each 40x40 mm², and an RoC of 900 mm, the FoV is 18.6x18.6° (0.1 sr) each. MCOs have been under development at the U. of Leicester and were used in the Mercury Imaging X-ray Spectrometer instruments (MIXS-C and MIXS-T) on BepiColombo [Fraser 2010], launched Oct 2018. **CCDs:** CCDs and front-end electronics (by MIT and Lincoln Lab) detect X-ray photon location and energy. Each focal plane assembly (FPA) is composed of a 3x3 array of 5x5cm CCDs operated at -60° C, tip/tilted to approximate the spherical focal surface of the MCOs. **TRL:** All ≥ 6

4.3 Infrared Visible UV Telescope (IVUT)

The IVUT will localize sources to 0.5 arcsec relative to nearby stars and perform 4-band photometry. The IVUT is a 70-cm telescope with two instrument channels: 1) a wide-field imager using dichroics to obtain images in 4 bands (0.2-2.5 μm) simultaneously onto three IR and one visible-UV detectors, and 2) a low-resolution ($\lambda/\Delta\lambda \sim 30$) slit spectrometer. **Telescope:** The Korsch 3-mirror anastigmat telescope provides well-corrected images over a wide FoV and an accessible exit pupil. The fold mirror behind the primary is mounted on a fast steering mechanism to provide the fine pointing stability requirement. A pickoff mirror and slit at the Cassegrain focus directs light into the spectrometer, while the offset imaging field continues to the tertiary mirror and aft-optics assembly (including the imager optics, spectrometer, and detectors.) **Detectors:** The 4 detectors are standard Teledyne H4RG (quan 3) and HiViSI (quan 1); 4Kx4K pixels each. The spectral channel is placed on the edge of one of the detectors. **Sensitivity:** using the 70 cm aperture, the PSF, the pointing jitter, budgeted wavefront error, a background of 4 times the ecliptic poles, telescope thermal emission, and read-noise, the flux limit for a flat spectrum source in a 300-s exposure is $AB \approx 23$ for all 4 bands. **TRL:** All ≥ 6.

4.4 X-ray Telescope (XRT)

The XRT (McClellan 2017) provides ~2 arcsec source localization, with deep sensitivity (5×10^{-15} erg/cm²/s in 2 ks), over a 1 deg diameter FoV. The large XRT FoV means that it can be used to search for X-ray counterparts to GW events, as well as function in a survey mode, probing deeply for transients. The XRT will also improve upon the WFI localizations. **Detector:** The detector assembly (TRL 6) is CCDs produced by MIT/LL. The focal plane array is 100x100 mm of CCDs (2x2 array) with 45μm 3x3 binned pixels (1.8"/pix). **Mirror:** The mirror assembly consists of 6000 single crystal silicon mirrors, each 100mm x 100mm x 0.4mm, resulting in a maximum diameter of 1.3 m. The mirrors are polished using a process developed at GSFC [Zhang 2018], and coated with 20 nm iridium to enhance X-ray reflectivity. They are assembled with silicon spacers and adhesive. **TRL:** now TRL 5; TRL 6 by 2021 (see §5).

4.5 Gamma-ray Transient Monitor (GTM)

The GTM provides all-sky detection of GRBs and other transients. **Detectors:** The GTM consists of 8 detectors mounted on the spacecraft and instrument section such that there is one detector pointed along the normal vector of each face of an octahedron. Each detector is a 20 cm

diameter by 1.27 cm thick disk of NaI(Tl) crystals with a Beryllium window (10 keV to 1 MeV bandpass) and photomultiplier tube (PMT). **Localization:** GRB localization is accomplished by using the off-axis variation in responsivity of the 4 detectors in the hemisphere centered on the GRB. The accuracy is < 10 degree radius. **Sensitivity:** A trigger from two of the 8 detectors plus background yields a sensitivity of 0.9 ph/cm²/sec (1 sec, 50-300 keV). **TRL:** All ≥ 6 .

4.6 TAP: A Next Generation Transient Observatory

The TAP mission provides a factor of ~ 10 improvement in instrument sensitivity and FoV compared to *Swift* (the current multi-band transient mission) (**Table 4**). In addition, TAP's L2 orbit ensures minimal ($\sim 10\%$) Earth occultation, enabling improved rapid response. TAP will use these improvements to support a large Guest Observer community in targeted and follow-up time-domain observations (see **Fig. 1**).

Table 4: Comparison of TAP to Swift

EM Band	<i>Swift</i>	TAP
X-ray (narrow)	XRT: FoV: 0.1 deg ² F _{lim} : 8×10^{-14} erg cm ⁻² s ⁻¹ (10 ks, 0.3-10 keV)	XRT: FoV: 0.8 deg ² F _{lim} : 5×10^{-15} erg cm ⁻² s ⁻¹ (2 ks, 0.2-10 keV)
X-ray (wide)	BAT: FoV: 1.4 sr F _{lim} : 6×10^{-10} erg cm ⁻² s ⁻¹ (2ks, 15-150 keV)	WFI: FoV: 0.4 sr F _{lim} : 2×10^{-11} erg cm ⁻² s ⁻¹ (2 ks, 0.4-4 keV)
UV - optical - IR	UVOT: FoV: 0.1 deg ² F _{lim} : 19 mag (300 sec, 0.16 - 0.7 micron)	IVUT: FoV: 1 deg ² F _{lim} : 23 mag (300 s, 0.2 - 2.5 micron)
Gamma-ray	BAT: FoV: 1.4 sr F _{lim} : 3.0×10^{-8} erg cm ⁻² s ⁻¹ (1 s)	GTM: FoV: 4π sr F _{lim} : 0.9 ph cm ⁻² s ⁻¹ (1 s)

5. Technology Development (for XRT)

There are 2 basic steps in building the XRT mirror assembly. As of January 2019, mirror segments (TRL 5) meeting all TAP/XRT requirements, including technical performance as well as schedule and cost, have been made repeatedly (first step). The basic technical elements of the second step, i.e., integration of mirror segments into mirror modules, have also been demonstrated by repeatedly aligning and bonding a pair of primary and secondary mirror segments and subject them to full-illumination X-ray tests, achieving 1.3" HPD X-ray images. **TRL Raising:** We are now preparing to build and test a mirror module with 12 pairs of mirror segments, requiring only new engineering. This mirror module will be subject to X-ray performance tests before and after a set of environmental tests, including vibration, acoustics, and thermal vacuum. Fully funded by NASA's ROSES Strategic Astrophysics Technology program, this process will be complete by 2021, achieving TRL-6.

6. Organization and Partnerships

TAP will be designed, built and managed at GSFC. GSFC will partner with U. Leicester on the design of the WFI, and MIT/Lincoln Lab on the design and production of the CCDs.

7. Project Schedule (developed by the GSFC Mission Design Lab)

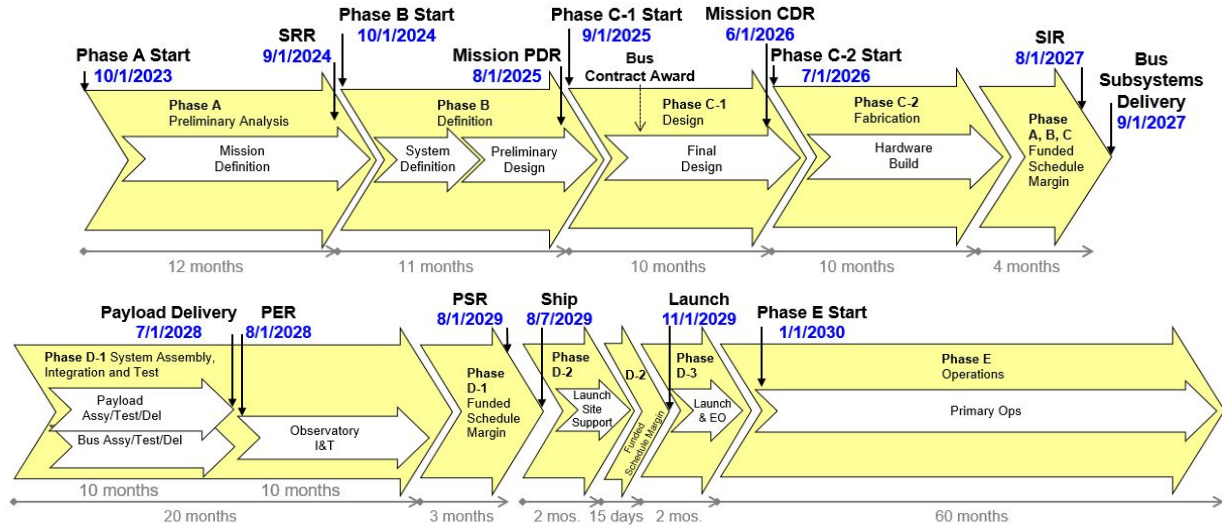


Fig 2: The TAP observatory schedule supports a Nov 2029 launch, given an Oct 2023 start date.

8. Cost Estimate and Methodology (based on 2018 GSFC Mission Design Lab run)

Table 5 shows the TAP mission costs, estimated with a GSFC CEMA parametric model (PRICE-H). The credibility of the estimate comes from two factors: 1) TAP requires minimal technology development (§5), thus most costs may be estimated directly from the hardware design; 2) there exists independent proposal heritage for the TAP instruments: ISS-TAO (WFI), Star-X (XRT), EXIST (IVUT), and actual cost heritage including IVUT (industry), spacecraft (*Swift*), and GTM (*Fermi-GBM*). The TAP mission cost of \$1070M is consistent with the Probe cost cap (\$1B), within the accuracy of the costing process (~15%.) This cost was verified by an independent GSFC Resource Analysis Office (RAO) estimate of \$975M (70% confidence level).

Table 5: Master Equipment List Based Parametric Total Lifecycle Cost Estimate (by GSFC CEMA 2018)

PROJECT PHASE	TAP WBS/Sub-system	TAP Mission COST [FY18 \$M]
Phase A		\$35
Phases B-D	Mgmt, Sys Eng, Mission Assur.	\$86
	Science (<i>to community</i>)	\$25
	X-ray Telescope (XRT)	\$70
	Wide-Field Imager (WFI)	\$91
	IR-Vis-UV Telescope (IVUT)	\$103
	Gamma-ray Trans Mon (GTM)	\$24
	Spacecraft, including ATLO	\$150
	Ground Data Systems	\$31
	Launch Vehicle and Services	\$150
	Reserves (30%)	\$230
	Total Cost Phases B-D	\$995
Phase E-F	Operations	\$66
	Reserves (15%)	\$10
	TOTAL LIFECYCLE COST	\$1,070

References

- Abbott, B. et al. (2017a)* “GW170817: Observation of gravitational waves from a binary neutron star inspiral”, PRL, 119, 1101
- Abbott, B. et al. (2017b)* “Multi-messenger observations of a binary neutron star merger”, ApJL 848, 12
- Abbott, B. et al. (2017c)*, “Gravitational waves and gamma-rays from a binary neutron star merger: GW170817 and GRB 170817A” ApJL, 848, L13
- Abbott, B. et al. (2018)* “Prospects for observing and localizing gravitational-wave transients with Advanced LIGO, Advanced Virgo and KAGRA”, Living Rev. in Relativity, 21, 3
- Angel, J. (1979)* “Lobster eyes as x-ray telescopes” ApJ 233 364
- Beckmann, V. & Schrader, C. R. (2012)* “Active Galactic Nuclei” ISBN-13: 978-3527410781. Wiley-VCH Verlag GmbH
- Baker, J. et al, “Multimessenger science opportunities with mHz gravitational waves”, Astro2020 Whitepaper
- Bowen, D. B. et al. (2018)* “Quasi-periodic behavior of mini-disks in binary black holes approaching merger” ApJL 853, 17
- Breedt, E. et al. (2010)* “Twelve years of X-ray and optical variability in the Seyfert galaxy NGC 4051” MNRAS, 403, 605
- Burns, E et al (2019)* “A summary of multi-messenger science with neutron star mergers” Astro2020 Whitepaper
- Burrows, D. N. et al. (2011)* “Relativistic jet activity from the tidal disruption of a star by a massive black hole” Nature 476, 421
- Cucchiara et al. (2011)* “A photometric redshift of $z \sim 9.4$ for GRB 090429B”, ApJ 736, 7
- Dal Canton et al. (2019)* “Detectability of modulated X-rays from LISA's supermassive black hole mergers” eprint arXiv:1902.01538
- D’Ascoli et al. (2018)* “Electromagnetic emission from supermassive binary black holes approaching merger” ApJ, **865**, 140
- Fong, W. et al (2015)* “A Decade of short-duration Gamma-ray Burst broadband afterglows: energetics, circumburst densities, and jet opening angles”, ApJ 815, 102
- Fraser, G. et al. (2010)* “The Mercury imaging X-ray spectrometer (MIXS) on BepiColumbo” Planetary & Sp.Sci., 58, 79
- Gezari, S. et al. (2008)* “UV/Optical detections of candidate tidal disruption events by GALEX and CFHTLS” ApJ, 676, 944
- Grindlay et al (2019)*, “GRBs as probes of the early universe with TSO”, Astro2020 Whitepaper
- Goldstein, A. et al. (2017)* “An ordinary short gamma-ray burst with extraordinary implications: Fermi-GBM detection of GRB 170817A”, ApJL, 848, 14
- Haiman, Z. (2017)* “Electromagnetic chirp of a compact binary black hole: A phase template for the gravitational wave inspiral”, [Phys Rev D, 96 023004](#)

- Kelley, L. et al (2019)* “Multimessenger astronomy with Pulsar Timing Arrays”, Astro2020 Whitepaper
- Körding, E.G., Migliari, S., Fender, R., et al. (2007)* “The variability plane of accreting compact objects” MNRAS, 380, 301
- Lien, A. et al. (2014)* “Probing the cosmic gamma-ray burst rate with trigger simulations of the Swift Burst Alert Telescope” ApJ 783, 24
- McClelland, R.S. et al. (2017)* “The STAR-X X-ray Telescope Assembly (XTA)” SPIE Proc. 10399, 1039908
- McHardy I. et al (2006)* “Active galactic nuclei as scaled-up Galactic black holes” Nature, 444, 730
- Metzger, B. (2017)* “Kilonovae” Living Reviews in Relativity, 20, Issue 1, 3, pp. 59
- Mingarelli et al. (2017)* “The local nanohertz gravitational-wave landscape from supermassive black hole binaries”, Nature Astronomy 1, 886
- Perlmutter et al. (1999)* “Measurements of Ω and Λ from 42 high-redshift supernovae”, ApJ 517, 565
- Rees, M. (1988)* “Tidal disruption of stars by black holes of 10^6 to 10^8 solar masses in nearby galaxies”, Nature 333, 523
- Riess et al. (1998)* “Observational evidence from supernovae for an accelerating universe and a cosmological constant”, AJ 116, 1009
- Salvaterra, R. et al. (2009)* “GRB 090423 at a redshift of $z \sim 8.1$ ” Nature, 461, 1258
- Sathyaprakash, B et al (2020)* “Multimessenger universe with gravitational waves from binary systems”, Astro2020 Whitepaper
- Schnittman, J. D. (2014)* “Coordinated observations with Pulsar Timing Arrays and ISS-Lobster” arXiv:1411.3994
- Tanvir, N. et al. (2009)* “A gamma-ray burst at a redshift of $z \sim 8.2$ ” Nature, 461, 1254
- Taylor, S. R., et al. (2016)* “Are we there yet? Time to detection of nanohertz gravitational waves based on pulsar-timing array limits” ApJL, 819, 6
- Troja, N., et al (2017)* “The X-ray counterpart to the gravitational-wave event GW170817”, Nature 551, 71
- URL 1: https://smd-prod.s3.amazonaws.com/science-red/s3fs-public/atoms/files/TAP_Study_Rpt.pdf
- URL 2: <https://dcc.ligo.org/LIGO-T1800133/public>
- van Velzen, S. et al. (2018)* “On the mass and luminosity functions of tidal disruption flares: rate suppression due to black hole event horizons”, ApJ, 852, 72
- Zhang, W. et al. (2018)* “Astronomical X-ray optics using mono-crystalline silicon: high resolution, light weight, and low cost”, SPIE Proc. 10699, 1069900

Acronyms

AGN	Active Galactic Nuclei	MCO	Micro-Channel Optic
ATLO	Assembly, Test, and Launch Operation	MDL	Mission Design Laboratory
BH	Black Hole	MEV	Maximum Expected Value
BNS	Binary Neutron Star	MIXS	Mercury Imaging X-ray Spectrometer
CEMA	Cost Estimating, Analysis, and Modeling Office (at GSFC)	MMA	Multi-Messenger Astronomy
CBE	Current Best Estimate	NaI	Sodium Iodide
CCD	Charge Coupled Device	NS	Neutron Star
ccSN	Core-collapse supernova	PM	Primary Mirror
EM	Electro-Magnetic	PMT	Photomultiplier Tube
FoR	Field of Regard	PTA	Pulsar Timing Array
FoV	Field of View	RAO	Resource Analysis Office (GSFC)
FPA	Focal Plane Assembly	RoC	Radius of Curvature
FWHM	Full Width at Half Maximum	ROSES	Research Opportunities in Earth and Space Science
GALEX	Galaxy Evolution Explorer	S/C	Spacecraft
GBM	Gamma-ray Burst Monitor (on <i>Fermi</i>)	sGRB	short Gamma-Ray Burst
GEVS	General Environmental Verification Standard	SKA	Square Kilometer Array
GRB	Gamma-Ray Burst	SM	Secondary Mirror
GSFC	Goddard Space Flight Center	SMBH	Supermassive Black Hole
GTM	Gamma-ray Transient Monitor	SNe	Supernovae
GW	Gravitational Wave	TAP	Transient Astrophysics Probe
HiViSI	Hybrid Visible Silicon Imager	TDE	Tidal Disruption Event
HPD	Half Power Diameter	ToO	Target of Opportunity
H4RG	Hawaii 4k, R is Reference pixels, and G is Guide windows	TRL	Technology Readiness Level
IPTA	International Pulsar Timing Array	UV	Ultraviolet
IVUT	Infrared/Visible/UV Telescope	UVOT	UV/Optical Telescope
JWST	James Webb Space Telescope	WFI	Wide-Field Imager
KAGRA	Kamioka Gravitational Wave Detector	WFIRST	Wide Field Infrared Survey Telescope
LIGO	Laser Interferometer Gravitational-wave Observatory	XRT	X-ray Telescope
LISA	Laser Interferometer Space Antenna		
LOFAR	LOW Frequency ARray		
LSST	Large Synoptic Survey Telescope		